bioresources.cnr.ncsu.edu

Characterization of Wood Fiber Insulation for the Development of Wood Fiber-Insulated Panels (WIPs) for Use in Building Envelope

Jacob Snow,[a,c] Benjamin Herzog,[a,*] Liam O'Brien,[b,c] and Ling Li [c,*]

Wood fiber insulation (WFI) was studied as an eco-friendly alternative for fossil-based building insulation, focusing on its use in new wood fiber-insulated panels (WIPs). Rigid WFI boards with densities of 110, 140, and 180 kg/m³, including a 140 kg/m³ variant without paraffin wax, were evaluated. Key properties investigated included porosity, water vapor transmission, liquid water adsorption, and thermal conductivity. The porosity ranged between 85 and 92%, primarily influenced by density. Water vapor permeability ranged from 65 to 90 ng·s^{-1}m^{-1}Pa^{-1}, while liquid water absorption was between 2.5 and 20% by volume, influenced by both wax and density. The thermal conductivity coefficient ranged from 0.038 to 0.055 W/(m·K). Bond strength tests with WFI (140 kg/m³ with wax) laminated to various materials using structural adhesives showed tensile perpendicular-to-grain strengths of 10 to 16 kPa and shear strengths of 60 to 90 kPa, with failure only occurring within the WFI. It was concluded that WFI is a promising material for novel WIPs, offering competitive hygrothermal properties and compatibility with structural adhesives. However, its bio-based nature suggests variability and complexity, necessitating further rigorous testing in various climates and in more complex assemblies.

INTRODUCTION

The built environment is responsible for 40% of global CO_2 emissions per year, which is equivalent to 14.6 gigatons of CO_2 per year. 9.9 gigatons of that 14.6 are directly related to building operations (Architecture 2030, 2021). In addition to the emissions related to buildings, industry consumes massive amounts of natural resources, and many of the materials used and produced in construction are detrimental to human health (Pacheco Torgal *et al.* 2012). One of the primary methods of addressing this problem is through modification of the building envelope. Improving the thermal envelope of a building can drastically reduce its operating carbon footprint. Prefabricated insulation panels with insulation and sheathing combined into a single panel is a popular and effective approach to addressing thermal loss by retrofitting existing buildings and building new envelopes. However, addressing this issue with fossil fuel-based insulation materials can be counterproductive to solving this problem due to the high embodied carbon of the

insulation. Polystyrene foam-based insulation materials, a common core for structural insulated panels (SIPs), can have an embodied carbon of 4.2 to 5.8 kg CO_2 per kg of material (Kunic 2017) and are formulated using non-renewable hydrocarbon oils. Further expansion of the built environment necessitates the importance of material selection, with the research, development, and utilization of bio-based alternatives being among the most impactful steps in mitigation of anthropogenic impacts on local and global environments.

Wood fiber insulation (WFI), see Fig. 1, is an insulation product manufactured from wood that has been fibrillated in either a wet or dry process (Veitmans and Grinfelds 2016). The fibers can be used in a loose form for blow-in insulation or formed into boards for a between stud or external-continuous-envelope and prefabricated applications. WFI is an environmentally friendly alternative material to carbon emitting materials; carbon sequestered by a growing tree is retained when the tree is processed into building materials and therefore stored for the life of the building (Lawrence *et al.* 2013). This negative carbon input is a critical factor when evaluating the equivalent CO_2 emissions associated with a building, given the massive volume of carbon that could potentially be sequestered in the building the built environment. The fibers used in the production of WFI can be sourced from a breadth of various species and/or timber processing residuals. This flexibility further improves the environmental impact of these materials by rerouting waste streams from landfills and furnaces and also improves timber basket markets by reducing difficult waste streams (O'Dwyer *et al.* 2018). WFI is non-toxic, which is important while handling and cutting the final product; this is in contrast to the irritating and toxic materials generated by traditional insulation materials (Stec and Hull 2011; Pacheco-Torgal *et al.* 2012). WFI performs similarly to other foams, such as expanded polystyrene (EPS) and extruded polystyrene (XPS), for certain properties, *e.g.*, thermal resistance, while offering advantages in other aspects, such as water vapor permeance. However, there are also some minor disadvantages to using WFI. It is less insulative but denser than other non-renewable options such as mineral wool. The same level of insulation can be achieved using WFI, but it requires a thicker layer. In order for the boards to be easily handled, they may need to be manufactured at densities several times that of foam boards. However, these drawbacks are manageable at an off-site manufacturing plant and/or job-site with proper planning.

Fig. 1. Wood Fiber Insulation Boards (TimberHP & Go Lab Inc. 2024, n.d.)

Structural insulated panels (SIPs) are a common solution for high performance buildings. These panels are prefabricated assemblies of two or three layers; a skin on one or both sides (typically oriented strand board a.k.a. OSB) with a core of XPS insulation. These layers are then affixed to each other with structural adhesives. If WFI board is used as a drop-in insulation panel to replace XPS/EPS in structural insulated panels (SIPs), retrofit insulated panels (RIPs), or used in novel wood fiber insulated panels (WIPs) (products currently being developed by the authors – see below), the bonding performance of WFI and wood-based skin materials, such as oriented strand board (OSB) and cross-laminated timber (CLT) panels, plays a vital role in maintaining the integrity of the final laminated products. There are a number of adhesives that can potentially be used to manufacture SIPs and RIPs; Phenol formaldehyde, polyurethane, polyether and isocyanate-based adhesives are just a few examples. These adhesives must be qualified for use under International Building Codes, specifically ICC-ES AC05 (ICC Evaluation Service 2020) in the U.S. However, there is a lack of adequate information addressing the bonding performance between wood fiber insulation and wood-based products. The open porous nature of the WFI may impact the bond strength as compared to standard bonding of wood to wood or wood to polyurethane foams, due to the increased absorbance of the adhesive prior to resin curing. This information could be critical to the successful development of all wood structural insulated panels and other novel adhesively bonded WFI assemblies.

In addition, the assessment of how building materials react when exposed to temperature and moisture gradients (generally referred to as "hygrothermal behavior") is critical to the successful estimation of building durability, operational energy efficiency, and occupant comfort (Cetiner and Shea 2018). If such hygrothermal properties of the materials are not assessed in a holistic way and the appropriate solutions integrated into building design, then the resulting building may suffer from excess energy use as a result of heat loss through the envelope, and inefficient indoor climate conditioning. The building may also experience structural damage from condensation within the insulation layer and elevated moisture content which, in turn, may lead to decay or mold causing poor indoor air quality and an unhealthy environment (Brambilla and Sangiorgio 2020). High performance buildings that are tight and have thick impermeable insulation layers are at particular risk as any moisture introduced cannot escape the envelope. This behavior considers the simultaneous and interdependent absorption, storage, and release, of both heat and moisture (Cetiner and Shea 2018). A porous hygroscopic building material, such as WFI in this study, after some period exposed to a given temperature and relative humidity, will reach a state of equilibrium with this environment, exchanging the water vapor in its pores with the ambient air. This equilibrium is also impacted by the current state of the material. If it is releasing moisture, then it will reach a different equilibrium than when it is gaining moisture. This phenomenon is a result of the interaction of liquid and vaporous water within the pores bonding with the material (Salonvaara 2004; Simonson *et al.* 2004a,b; Hameury 2005; Osanyintola *et al.* 2006; Meissner *et al.* 2010; Belakroum *et al.* 2017). These bonds also impact the movement of energy through the material as the bonds take energy to form and release energy as they break (Faghri and Zhang 2006; Koizumi *et al.* 2017). At the assembly level and whole building level, the hygrothermal performance and energy consumption of building envelopes with different configurations and in various climate zones are simulated by solving combined heat and moisture transfer equations using WUFI and EnergyPlus software (Karagiozis *et al.* 2001; Ciancio *et al.* 2018). Specifically, the input material properties have a large influence on

the reliability and accuracy of the modeling results.

This study aimed to conduct material characterizations of WFI materials as an alternative to fossil-based building insulation materials, targeting SIPs, RIPs, and WIPs. A better understanding of these material properties, and potential benefits, will serve to derisk their use, thereby accelerating market acceptance. As part of this work, the hygrothermal properties and physical properties of WFI rigid boards having three densities (110, 140, and 180 kg/m^3) and one (140 kg/m^3) without paraffin wax treatment were evaluated following relevant ASTM standards. Properties evaluated included: porosity, water vapor permeability, liquid water retention, and thermal conductivity. Each of these properties influence how the insulation acts in a building and their use conditions. Porosity, being the volume of a material that consists of open spaces, directly influences moisture, air, and thermal relations. Water vapor permeability, the speed at which water vapor passes through a given thickness of material, plays a critical role in the design of a building envelope and is listed with most building envelope products. Liquid water retention, the weight and volume of water retained by the material, can be used to prescribe use conditions and hazards when handling the material. Lastly, the thermal conductivity, the amount of energy required to raise the temperature of a given area of material, is the single most heavily weighted factor when designing a building envelope.

The second part of this work evaluated the bonding performance of a representative WFI product (140 kg/m^3, with wax) with two face materials, lumber and OSB, bonded with three structural adhesives (a two-part emulsion polymer isocyanate and two types of one-component polyurethane). As described in detail below, materials were laminated and tested for tensile perpendicular-to-grain bond strength and shear strength to ensure adequate bonding of WFI to other wood-based materials could be achieved.

EXPERIMENTAL

Materials

The WFI materials used were sourced from a European manufacturer and made using a dry process. The boards were formulated from softwood fibers and pressed into boards after a mix of adhesive and other additives, often water repellants or fire retarders, were introduced onto the dry fibers. The WFI boards were manufactured with polymeric methylene diphenyl diisocyanate (pMDI). Some of the boards had paraffin wax as an additive to reduce the water uptake (Kirsch *et al.* 2018; De Ligne *et al.* 2022). The panels had nominal densities of 110, 140, and 180 kg/m^3 with a variant of the 140 boards without paraffin wax, as shown in Table 1. Those selected are representative of densities commonly used for continuous wall envelopes in the building industry. The nominal thicknesses of the insulations were as follows, 38 mm for the 110 and 180 boards and 60 mm for the 140 boards. The moisture content of WFI panels as received was within the range of 7% to 9%. Type IX EPS insulation, 35 kg/m^3 density, was purchased from a local contractor for comparative testing in a portion of the physical properties testing. OSB panels, having a nominal thickness of 11 mm, were sourced from a local retailer. The OSB was manufactured with Southern Yellow Pine wood strands, pMDI adhesive, and wax to manage moisture. The moisture content of OSB was $9.8 \pm 0.2\%$ (mean±sd), and the corresponding density of the OSB was 601 ± 20 kg/m^3. Dimensional lumber, a commercial mix of spruce, pine and fir (SPF-S), was used in this study to simulate bonding WFI to a CLT panel. The lumber was conditioned to ~12% moisture content prior to use. The density of lumber samples at $11.7 \pm 0.6\%$ MC was 337 ± 6 kg/m^3.

Table 1. List of Materials Used as Substrates

Materials	Nominal Density (kg/m^3)	MC (%)	Nominal Thickness (mm)	Wax	Code
WFI	110	7.5	38	Y	110W
	140	7.5	60	Y	140W
	140	8.45	60	N	140NW
	180	7.5	38	Y	180W
OSB	600	9.8	11	Y	OSB
Lumber	340	11.7	35	N	SPF

Three adhesives were tested: a two-part Emulsion Polymer Isocyanate (EPI) (used in manufacturing various engineered wood products such as MDF and plywood) and two types of polyurethane (PUR) adhesives. "PUR-R" is a rapid set single component polyurethane (PUR) adhesive commonly used for SIP manufacturing, and "PUR-S" is a slow set single component polyurethane adhesive commonly used for engineered wood products. The application information of adhesives is summarized in Table 2.

Table 2. Types of Adhesives

Adhesive	Code	Primer	Application Rate, g/m^2	Press time
Polyurethane	PUR-S	Yes	249	2 h
Polyurethane	PUR-R	Water	215	8 min
Emulsion Polymer Isocyanate	EPI	No	245	16 h

Porosity of WFI

The porosity of WFI samples was determined using the skeletal volume [defined as the sum of the volumes of the solid material and closed (or blind) pores within the material (if any)] and the envelope volume, *i.e.*, the sum of the volumes of the solid material and all types of pores within the material, of a sample. The nominal dimensions of WFI samples were 2.54 x 2.54 x 7.62 cm. The four WFI types were 110W, 140W, 140NW, and 180W. Before testing, all samples were oven-dried to prevent any moisture from influencing the test results. The skeletal volume of WFI was determined with a gas pycnometer (AccuPyc II 1340, Micromeritics), which measures the skeletal volume of a material by gas (helium) displacement using the volume-pressure relationship of Boyle's Law. The operation of the gas pycnometer followed the instructions provided by Micromeritics. This subtractive method provides the closest approximation of skeletal volume for a porous material (Donato and Lazzara 2012). The apparent volume of WFI was measured using a digital caliper. The measurement of both skeletal volume and true volume was repeated three times for each sample with three replicates of each material type.

Water Vapor Permeability of WFI

The water vapor transmission rates of three densities of WFI, a variant of WFI without paraffin wax and EPS were evaluated following ASTM E96/E96M Test Methods for Gravimetric Determination of Water Vapor Transmission Rate of Materials (2022). The apparatus used was a straight-sided, circular glass bowl with the samples cut to press fit into the cups. To eliminate the influence of edge width of wax sealing, which is normally applied to the top surface of the sample, on the water vapor permeability of the samples, a modified method was used to assemble the sample. With this method, the edges were sealed with vacuum grease to prevent moisture penetration and press fit into a glass container.

Examples can be seen in Fig. 2. This change eliminated the need to adjust for edge effect in the final results, which is especially critical for these samples given their thickness. The samples were conditioned to 21 °C and 50% RH until mass reached a constant value, less than 1% change over two hours, and then tested at those same conditions to minimize weight changes resulting from moisture content changes in the material as opposed to moisture transfer into the silica desiccant. Prior to the start of the test, the full assemblies were weighed as a zero-hour measurement. The samples were then placed in an environmental chamber set to 21 °C and 50% RH and weighed every 24 h for 10 days. A standard triplicate was used with a fourth specimen being a blank to determine if any adjustment to the slope was needed for sample weight changes. The weight measurements were plotted, and then the predicted slope for the trendline was used to calculate the water vapor transmission rate (WVTR). The differential in relative humidity and a saturation vapor pressure of 2.489 kPa at 21 °C was used to convert WVTR to water vapor permeance (WVP). The results were adjusted for the permeability of the still air in the cup and the surface resistance. Permeability was then calculated by multiplying the WVP by the thickness of the sample. The calculation of WVTR, WVP, and permeability of WFI samples followed the equations in ASTM E96.

Fig. 2. Permeability samples

Water Retention of WFI

The water retention of the wood fiber insulation was tested following ASTM C1763 *Test Method for Water Absorption by Immersion of Thermal Insulation Materials* (2020b). The dimensions of the samples were measured at 4 different points using a digital caliper for length and width, and at 12 locations for depth. Finally, they were weighed immediately prior to being fully submerged below 12.7 mm of water for two hours. The samples were removed from the water and allowed to drain on end for 10 min. At that point, any remaining surface water was dabbed away with paper towels, and the samples were measured to find the percent water retained as a ratio of the original weight and the original volume. WFI samples with three replicates of each included 110W, 140W, and 180W, as well as 140NW and Type IX EPS. The EPS was tested using ASTM C1763*, Procedure B* along with the other WFI samples, despite *Procedure C* being standard for petroleum-based insulation. This was done to enable a true one-to-one comparison of the results.

Thermal Conductivity of WFI

The thermal conductivity of WFI samples was measured with a heat-flow meter (HFM) (HFM M446, Netzsch, Germany) following ASTM C518-21 *Test Method for Steady-state Thermal Transmission Properties by Means of the Heat Flow Meter*

Apparatus (2021a). The HFM measures the thermal conductivity of materials by controlling the temperature on each side of the material with two plates and then measuring the heat flux through the material and using entered values about the materials dimensions to convert the measured heat flux to thermal conductivity.

WFI samples (110W, 140W, 140NW, and 180W) were tested to develop a baseline of performance. The nominal dimensions of WFI samples were 30.5 cm (width) x 30.5 cm (thickness) x initial thickness. They were tested at an average temperature of 23.9 °C and a delta T of 22 °C, stipulated in ASTM C1058-03 *Practice for Selecting Temperatures for Evaluating and Reporting Thermal Properties of Thermal Insulation* (2010). The selection of the average temperature and a delta T was to mimic the building envelope containing WFI being used in a moderate climate. Two replicates were tested for the board at each density. For each variant the sample was tested twice by turning over and reweighing the sample.

An additional round of testing was conducted using 140NW WFI board and type IX EPS board as a control. This testing was more comprehensive with temperatures ranging from 0 to 60 °C at increments of 11 °C and a constant delta *T* of 22 °C. The intent of the experiment was to investigate the correlation of temperature and thermal conductivity of insulation, mimicking the applications in different climate zones and assemblies, for instance, from freezing to the mid-range of temperatures experienced under asphalt shingles (Rose 1992; Winandy and Hatfield 2007). For each material type, three replicates of each were tested, each sample being tested twice, with the sample being turned over for the second test. The nominal dimensions of samples were 305 mm (width) x 305 mm (length) x 102 mm (thickness). For the hygroscopic WFI board, the samples were placed back to condition in the environmental chamber (21 °C and 55% RH) for 24 h between each test to allow that each replicate had the moisture content recovered at the beginning.

Adhesive Bond Strength Testing of WFI, Lumber, and OSB for WIPs Development

A catalog of wood-based building products; multi-component Wood-fiber Insulated Panels (WIPs) comprised of a WFI core and engineered wood face(s) or skin(s) for prefabricated modular construction and retrofit applications are currently being developed by the authors. This suite of building products is envisioned to be engineered for specific application – both energy/insulative and structural – requirements.

Highly energy efficient exterior wall and roof assemblies are being designed for repeatable, yet customizable, building solutions. In one embodiment, one WIP face is cross-laminated timber (CLT) providing high structural strength and thermal mass. An opposite face is OSB supplying a low-cost nailable surface suitable for cladding attachment and serving as a water vapor barrier (WVB). The core is comprised of WFI providing a continuous thermal envelope for the structure. The panel components are bonded together using structural adhesives. An investigation of the lamination bondlines, in terms of manufacturing and performance, is described below.

Substrate Preparation

Three test assemblies were made, one with OSB bonded to WFI, one with WFI bonded to lumber, and a third with WFI bonded to WFI. Isolating these three bondlines was done to find out whether any specific bondline within the proposed WIP assembly would pose a problem for the strength of the entire composite panel. Two replicate panels

were made using each adhesive.

Prior to gluing, all substrate surfaces were prepared. The lumber was planed, removing 1.6 mm from each side, to guarantee a fresh bonding surface. Planing, instead of sanding, was done in order to keep the pores of the wood open, thus allowing for greater adhesive penetration and an improved bond strength. The lumber was then edged and cut to length, squaring the material and setting the dimensions to 178 mm x 610 mm. The WFI and OSB were sanded using a rotary drum sander, since planing was not a practical option for those materials. Material was removed just to the point that the entire surface was affected by a single pass, <1.6 mm. The insulation and OSB were then also cut to 178 mm x 610 mm. These initial preparations were performed in batches, guaranteeing that each panel's materials were prepared within an hour of gluing/pressing.

A hydraulic press was used to fabricate the test samples; a pressure of 455 kPa was selected. This pressure was the result of initial work done in conjunction with one of the adhesive manufacturers to determine the maximum pressure that could be applied while minimizing the deformation of the WFI. For each adhesive, the highest recommended spread rate was used to combat the high absorbency of the WFI. All the manufacturers' application/assembly recommendations were followed for the specific adhesives systems. Primer and water, when applicable, were applied using an aerosolizing paint sprayer, and the adhesives were applied using a squeeze bottle to simulate an extruded adhesive bead commonly found in commercial manufacturing. Both applications were controlled by placing the substrate on a scale and measuring the added mass of primer/adhesive. After pressing, the panels were cured for over 24 h.

Bond Strength Test Specimen Preparation

The tensile perpendicular-to-grain bond testing samples were cut to approximately 50.8 mm x 50.8 mm following ASTM C209 *Test Methods for Cellulosic Fiber Insulating Board* (2020). The samples were affixed to aluminum testing blocks of equal size using a hot melt adhesive. The shear samples were cut to approximately 50.8 mm x 38.1 mm following ASTM D905 *Test Method for Strength Properties of Adhesive Bonds in Shear by Compression Loading* (2021).

Fig. 3. Tensile perpendicular-to-grain testing (left) and shear testing (right) with a WFI:SPF Sample

Tensile Perpendicular-to-grain Bond Testing

The tensile perpendicular-to-grain bond strength testing was performed following ASTM C209 (2020). The testing was done in a hydraulic testing frame with a 22.7-kg calibrated load-cell and a loading rate of 51 mm /min as required in Section 13.3 of ASTM

C209. The samples were mounted to the frame using chains on the top and bottom of the samples perpendicular to the surface allowing the sample to self-align as tension was applied (Fig. 3, left).

Shear Strength Testing

The shear strength testing was performed following ASTM D905 (2021). As shown in Fig. 3 right, the samples were tested in a guillotine shearing tool mounted to a hydraulic testing frame with a 45.3 kg. calibrated load-cell. The loading rate used was 5 mm/min as required in Section 10 of ASTM D905.

RESULTS AND DISCUSSION

Porosity

The results of the porosity tests conducted on four different types of WFI samples using a gas pycnometer are presented in Table 3. The WFI sample with the lowest density of 110 kg/m^3 had the highest porosity of approximately 92%. As the density increased to 140 kg/m^3 and 180 kg/m^3, the porosity of WFI decreased to approximately 90% and 85.6%, respectively. The addition of paraffin wax had a minimal effect on the porosity of the WFI samples, as shown in the comparison of the 140W and 140NW WFI samples. The porosity of insulation materials is crucial for thermal conductivity, water retention, water vapor permeability, and structure stability, which is discussed in the relevant subsections below.

Table 3. Porosity Results of Four WFI Samples

WFI Samples	Apparent Volume (cm^3) (mean±sd)	Skeletal Volume (cm^3) (mean±sd)	Porosity (%) (mean±sd)
110W	32.02±0.82	2.52±0.04	92.1±0.26
140W	29.26±1.02	2.91±0.19	90.1±1.03
140NW	33.00±3.33	3.11±0.19	90.5±1.63
180W	29.79±0.36	4.28±0.03	85.6±0.17

Water Vapor Permeability Results

The results of water vapor permeability of all specimens after air gap correction are shown in Fig. 4. Overall, the four types of WFI specimens tested had much higher water vapor permeability than EPS, which is classfied as water vapor impermeable material (Schiavoni *et al.* 2016). Increasing the WFI's density resulted in the decrease of water vapor permeability. However, a great decrease was only observed when the density was increased from 140 to 180 kg/m^3; from above 90 to 65 ng·s^{-1}m^{-1}Pa^{-1}. Moreover, the porosity results in Table 3 supports this statement because the porosity of WFI at 110 kg/m^3 was comparable to that with 140 kg/m^3, both of which were greater than that of 180 kg/m^3 by about 6%.

As for the parafin wax treatment, the treatment also caused a slight decrease in the water vapor permeability. The results in this study are comparable with published data (Palumbo *et al.* 2016), who reported that wood fiber insulation rigid boards with a densitsy of 210 kg/m3 and a porosity of 86% had a water water vapour permeability of 30 ng·s^{-1}m^{-1}Pa^{-1} (dry cup) and 47 ng·s^{-1}m^{-1}Pa^{-1} (wet cup).
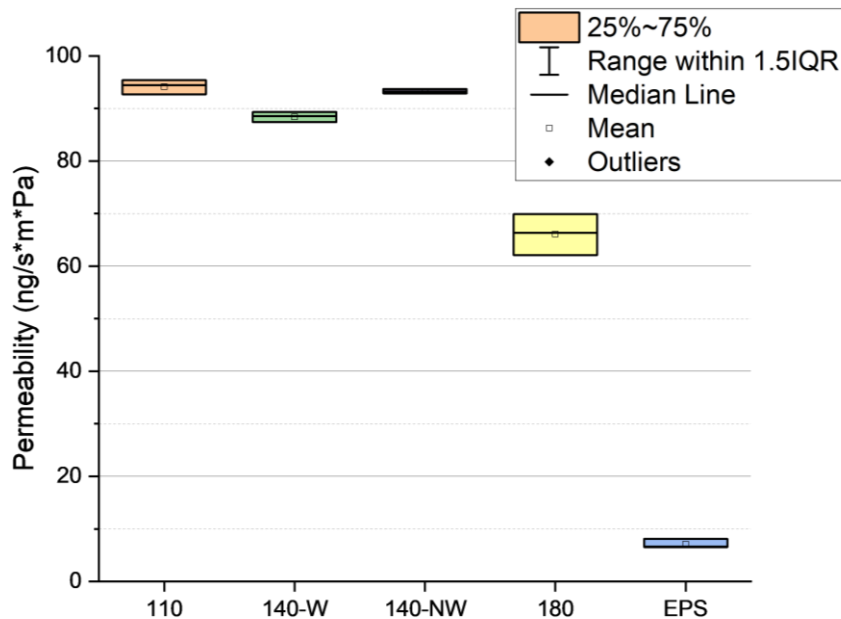
Fig. 4. Adjusted average permeability of insulation samples grouped by density

Water Retention Results

The water retention results of several insulation materials (110W, 140W, 140NW, 180W, and EPS as a control) are represented in two ways; as a ratio of initial weight (Fig. 5, left) and as a ratio of initial volume (Fig. 5, right). All the samples were tested under the same conditions. The absorption represented as a percentage of weight ranged from 15 to 122% across the four WFI variants. The EPS ranged from 25 to 52% within the sample of three. This variation is likely due to differences in the surfaces of the EPS. A small crack could enable a significant change in the percent difference while not being readily visible.

These results are in line with those reported by Muthuraj *et al.* (2019). Their study investigated four different bio-based insulation boards. The percent absorption ranged from 20 to 60% after two hours, with the wood fiber-based panel absorbing 55%. The panels tested did not include any wax but had high density, 454 kg/m^3. The WFI's performance was significantly impacted by the presence or absence of paraffin wax, with a ~200% increase in both weight and volume for the material without wax. The comparative relationship remained the same between weight and volume absorption apart from EPS. The EPS retained more water on a weight basis than both 110W and 180W but retained the least water on a volume basis. This variation was expected, given that the EPS has a density as low as 35 kg/m^3.

The increase in the 140W as compared to the other waxed WFI products is likely a result of production differences as the different densities are marketed as independent products for differing applications *i.e.* sarking boards or roof boards. This testing revealed that the inclusion of wax is critical to WFI's ability to manage bulk moisture, enabling it to perform similarly to petroleum-based insulation products. This reduces the risk of wetting events during or after construction significantly impacting wood fiber insulated buildings, especially when considered in conjunction with the permeability results previously discussed.
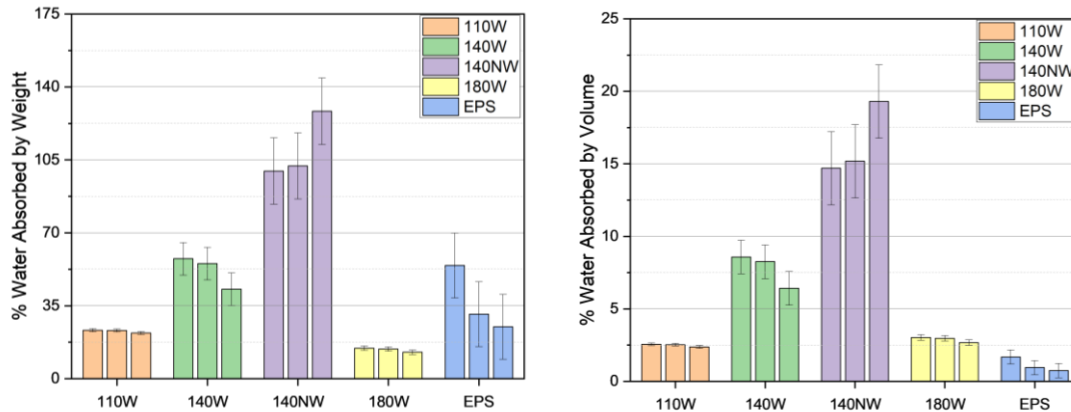
Fig. 5. Water retention as a ratio of initial panel weight (left) and a ratio of initial panel volume (right) of various insulation materials

Thermal Conductivity Results

The thermal conductivity results shown in Table 4 suggest a steady trend of increasing thermal conductivity as the density of the WFI increased. The thermal conductivity changed from 0.038 to 0.048 (W/(m·K)) as density increased from 110 to 180 kg/m^3. However, the thermal conductivity mean value of WFI with a density of 180 kg/m^3 was only slightly higher than that of WFI with a density of 140 kg/m^3, indicating the interchangeable use of these two WFI boards. Overall, the thermal conductivity results of WFI samples agree well with previous testing performed by multiple researchers (Cetiner and Shea 2018; Lawrence *et al.* 2013; Schiavoni *et al.* 2016; Veitmans and Grinfelds 2016).

Table 4. Single Condition Thermal Property Testing per ASTM C518

Thermal Conductivity Coefficient (λ), W/(m·K)	WFI Samples				EPS Samples
	110W	**140W**	**140NW**	**180W**	
Mean	0.038	0.047	0.048	0.048	0.035
SD	1.82E-4	3.29E-4	6.50E-03	1.37E-4	1.02E-04
COV	0.48%	0.70%	13.59%	0.28%	0.30%

Note: All samples were tested at an average temperature of 23.9°C and delta T of 22°C.

WFI is classified as a hygroscopic material, while EPS is hydrophobic. The moisture present in WFI(6 to 8% moisture content) can contribute to the overall thermal conductivity of WFI and alter it as the surrounding temperature fluctuates (Lawrence *et al.* 2013; Vololonirina *et al.* 2014; Cetiner and Shea 2018). Testing the hydrophobic EPS and hygroscopic WFI to evaluate the impact of temperature on thermal conductivity illustrated two different effects, as can be seen in Fig. 5. As the mean temperature increased from 11°C to 30°C, the thermal conductivity increased, which is in line with the results reported by Cetiner and Shea (2018) and Vololonirina (2014). When the mean temperature was above 30 °C, the thermal conductivity of the WFI decreased (Fig. 6, left). This indicates that the heat flow meter detected less heat flow. This may happen because some of the heat was being used to dry the moisture in WFI. Comparatively, a nearly linear increase in thermal conductivity of EPS with temperature was observed (Fig. 6, right). The moisture content of WFI may be driven down by the increase in temperature which combatted the steady rise of the thermal conductivity related to that same increase in temperature. This effect can be used to justify the implementation of natural insulation materials even in high

performance environments where extreme heat is regular. It is important to note that the thermal conductivity of WFI can increase up to 10% and decrease up to 15% before and after the mean temperature surpasses the threshold. Accounting for this change in the energy consumption analysis would lead to a more accurate estimation of energy use when the WFI is used in a building envelope.
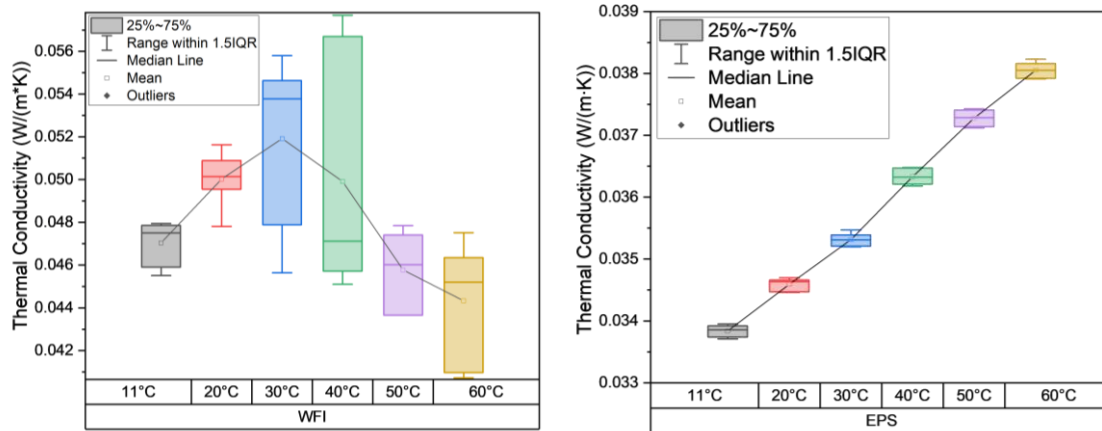

Fig. 6. Thermal Conductivity Coefficient of WFI (left) and EPS (right) from 11 to 60°C Mean Temperature

Tensile Perpendicular-to-grain Bond Strength

The box plot of tensile perpendicular-to-grain bond strength results of all the nine groups of specimens is shown in Fig. 6. The mean values of tensile strength of all groups were in the range of 10 to 16 kPa, two of which (WFI:OSB bonded with PUR-R and WFI:WFI bonded with PUR-S) had an outlier with an extremely low value. Outliers are shown in Figs. 7 and 8 but were excluded from the statistical analysis. The tensile strength results in this study are in line with the data reported by Euring *et al*. (2015). In that study, the tensile results of two types of WFI boards made of European spruce (*Picea abies*) (200 kg/m^3) ranged from 10 to 16 kPa, differing from fiber treatment methods (inactivated laccase-mediator-system in buffer and laccase in buffer) and drying processes (steam-air mixture, hot-air, and hot-air/hot-steam).

A two-way ANOVA analysis was conducted to examine the effects of adhesive type and substrate type on the tensile strength. The statistical analysis results showed that there was a statistically significant difference caused by adhesive type and specimen bond type (p-values of 6.10E-4, and 0.01, respectively). The mean comparisons analysis revealed that the mean of WFI:WFI bonds was statistically different from another two types of bonds: WFI:OSB and WFI:SPF. It also showed that the mean value of PUR-S adhesive type was statistically different from PUR-R and EPI. The means comparison results can be seen in Tables 5 & 6. The ANOVA statical analysis results are available upon request.

Table 5. Adhesive's Grouping Letters Table in Terms of Tensile Perpendicular-to-Grain Strength (Tukey HSD)
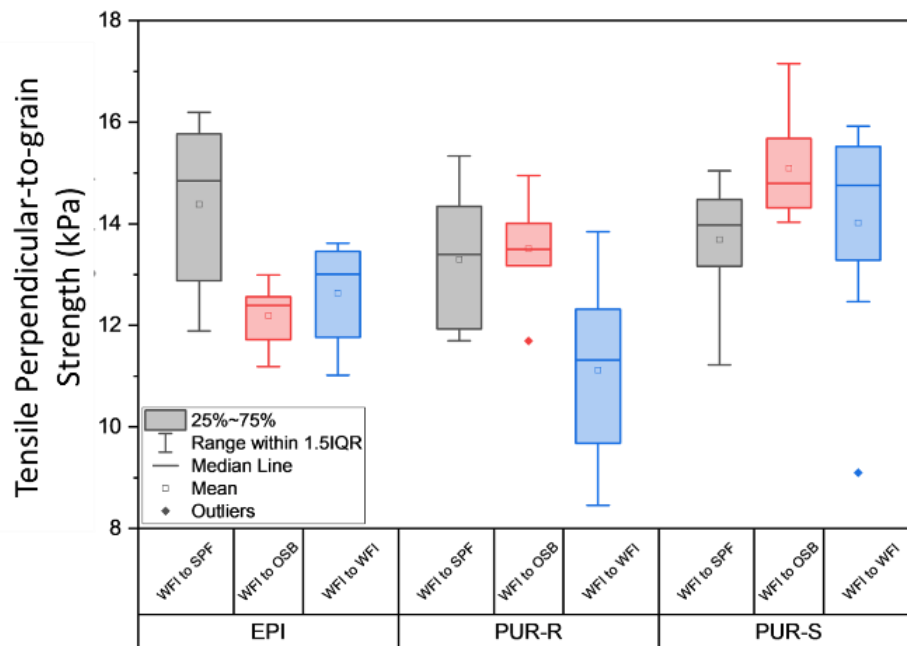
Adhesive	Mean (kPa)	Groups	
PUR-S	14.266	A	
EPI	13.069		B
PUR-R	12.603		B
Means that do not share a letter are significantly different.			

Table 6. Lamina's Grouping Letters Table in Terms of Tensile Perpendicular-to-Grain Strength (Tukey HSD)

Bond Type	Mean (kPa)	Groups	
WFI to SPF	13.788	A	
WFI to OSB	13.602	A	
WFI to WFI	12.590		B

Means that do not share a letter are significantly different.

Fig. 7. Summary of tensile perpendicular-to-grain bond results

Shear Strength

A box plot of shear strength results of all the nine groups of specimens is shown in Fig. 8. The mean values for all nine groupings were in the range of 60 to 90 kPa. Two groupings contained outliers significantly above average (WFI:SPF bonded with PUR-R and WFI:OSB bonded with EPI). These outliers are a result of the adhesive expanding into the WFI far enough that during loading in the shear fixture the interphase of the adhesive film and the substrate was loaded as opposed to purely loading the bondline. These outliers were excluded from the statistical analysis of the sample. A two-way ANOVA analysis was conducted to examine the effects of adhesive type and substrate type on the shear strength. The statistical analysis results showed that there was a statistically significant difference caused by adhesive type (p-value of 0.04); however, lamina type and the interaction of these two variables was not significant (p-values of 0.40, and 0.16, respectively). The mean comparisons analysis revealed that there was no entirely unique group among all the variables tested. The only variables that did not share a mean were the PUR-S and EPI adhesives. However, both shared a mean with the PUR-R adhesive. The results of the mean analysis can be seen in Tables 7 and 8. The full ANOVA statical analysis results are available upon request. A review of the literature did not reveal any existing data related to the shear performance of WFI when loaded in this manner. In-plane shear testing has been investigated on polyurethane-based SIPs, and the SIPs had a reported shear strength of

64.25 kPa with the same reported failure modes, all in the core (Kermani 2006). These data will be crucial in evaluating the feasibility of WIP assemblies for wall applications.

Table 7. Adhesive's Grouping Letters Table in Terms of Shear Strength (Tukey HSD)

Adhesive	Mean (kPa)	Groups	
PUR-S	75.932	A	
PUR-R	69.874	A	B
EPI	69.412		B

Means that do not share a letter are significantly different.

Table 8. Lamina's Grouping Letters Table in Terms of Shear Strength (Tukey HSD)

Bond Type	Mean (kPa)	Groups
WFI to WFI	73.586	A
WFI to SPF	71.775	A
WFI to OSB	69.937	A

Means that do not share a letter are significantly different.
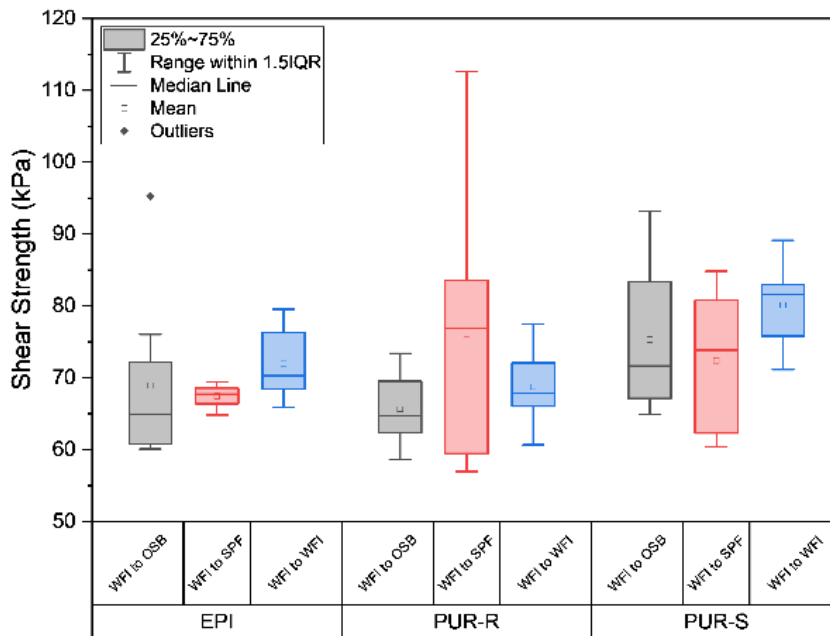
Fig. 8. Summary of shear strength results of specimen tested

Failure Mode of Bond Line for Tensile Perpendicular-to-Grain Bond and Shear Strength Testing

The adhesive did not control the strength of the total composite for any of the specimens tested for tensile perpendicular-to-grain bond and shear strength testing; 100% wood failure in WFI was observed in all the samples (Fig. 9). In this study, the adhesive application approach ensured adequate bonding performance, regardless of adhesive type and specimen bond type. This was the expected result for this testing as the low-density WFI boards have a very low internal bond and shear strength compared to the other components of WIP panels, *e.g.*, CLT, and OSB.
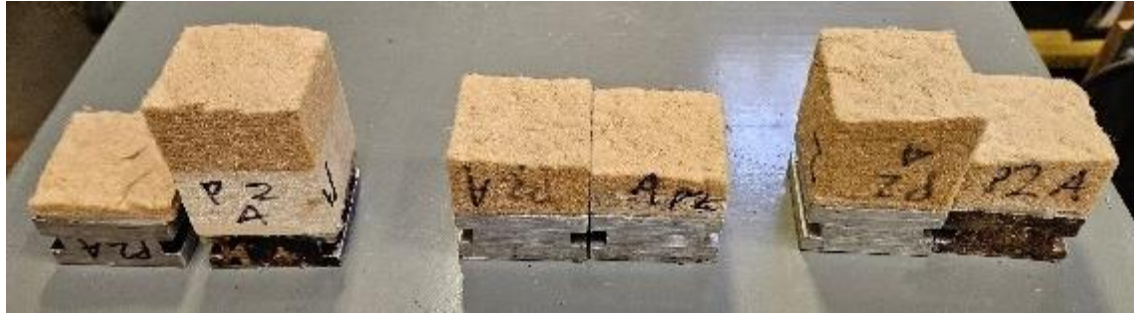
Fig. 9. Broken tensile perpendicular-to-grain bond test samples (left: WFI and Lumber; Middle: WFI and OSB; right: WFI and WFI)

CONCLUSIONS

1. The hygrothermal characteristics of wood fiber insulation (WFI) were thoroughly examined to gain an understanding of how these materials would perform in various climates and in the event of major wetting. Furthermore, the bond strength between WFI, lumber, and oriented strandboard (OSB) was tested using three types of structural adhesives. This information will help prevent shear failure and ensure load support requirements are met when determining the total weight of insulation, nail bed, and cladding, for example, in a wall assembly utilizing WFI. The analysis of these early-stage prototypes will ease the process of industry adoption of these novel materials and provide a basis for further research in the utilization of bio-based insulation as a mainstream building material.

2. Novel all-wood structural panel composites, such as WIPs, offer a compelling answer to the dual-edged problem of addressing emissions in the built environment. WFI has similar or superior properties compared to fossil-based insulation materials that are currently dominating the insulation market in terms of thermal conductivity, structural stability, and moisture management, while also being a carbon sink. The use of adhesives to prefabricate the wall assembly panels could further reduce the cost of materials and remove the thermal bridging effect of mechanical fasteners. The research findings serve as a baseline for the hygrothermal performance of WFI insulation materials, enabling further research into the performance of the total composite system and the impact of the adhesive layer. In particular, the composites must be evaluated for creep behavior, and the impact of the adhesive layer on total assembly permeability.

ACKNOWLEDGMENTS

London, SFR Laboratory Operations Manager, and Lilli Burrill, undergraduate research assistant, for their assistance with sample preparation and testing.

Legal Disclaimer

This report was prepared as an account of work sponsored by an agency of the United States Government. Neither the United States Government nor any agency thereof, nor any of their employees, makes any warranty, express or implied, or assumes any legal liability or responsibility for the accuracy, completeness, or usefulness of any information, apparatus, product, or process disclosed, or represents that its use would not infringe privately owned rights. Reference herein to any specific commercial product, process, or service by trade name, trademark, manufacturer, or otherwise does not necessarily constitute or imply its endorsement, recommendation, or favoring by the United States Government or any agency thereof. The views and opinions of authors expressed herein do not necessarily state or reflect those of the United States Government or any agency thereof.

REFERENCES CITED

Architecture 2030. (2021). "Why the built environment – Architecture 2030," (https://www.architecture2030.org/why-the-built-environment/).

ASTM C1058/C1058M (2010). "Practice for selecting temperatures for evaluating and reporting thermal properties of thermal insulation," ASTM International, West Conshohocken, PA.

ASTM C209 (2020). "Test methods for cellulosic fiber insulating board," ASTM International, West Conshohocken, PA.

ASTM C1763 (2020). "Test method for water absorption by immersion of thermal insulation materials," ASTM International, West Conshohocken, PA.

ASTM C518 (2021). "Test method for steady-state thermal transmission properties by means of the heat flow meter apparatus," ASTM International, West Conshohocken, PA.

ASTM D905-08 (2021). "Test method for strength properties of adhesive bonds in shear by compression loading," ASTM International, West Conshohocken, PA.

ASTM E96/E96M (2022). "Test methods for gravimetric determination of water vapor transmission rate of materials," ASTM International, West Conshohocken, PA.

Belakroum, R., Gherfi, A., Bouchema, K., Gharbi, A., Kerboua, Y., Kadja, M., Maalouf, C., Mai, T. H., El Wakil, N., and Lachi, M. (2017). "Hygric buffer and acoustic absorption of new building insulation materials based on date palm fibers," *J. Build. Eng.* 12, 132-139. DOI: 10.1016/j.jobe.2017.05.011

Brambilla, A., and Sangiorgio, A. (2020). "Mould growth in energy efficient buildings: Causes, health implications and strategies to mitigate the risk," *Renewable Sustainable Energy Rev.* 132, article 110093. DOI: 10.1016/j.rser.2020.110093

Cetiner, I., and Shea, A. D. (2018). "Wood waste as an alternative thermal insulation for buildings," *Energ. Build.* 168, 374-384. DOI: 10.1016/j.enbuild.2018.03.019

Ciancio, V., Falasca, S., Golasi, I., Curci, G., Coppi, M., and Salata, F. (2018). "Influence of input climatic data on simulations of annual energy needs of a building: EnergyPlus and WRF modeling for a case study in Rome (Italy)," *Energies* 11(10), 2835. DOI: 10.3390/en11102835

De Ligne, L., Van Acker, J., Baetens, J. M., Omar, S., De Baets, B., Thygesen, L. G., Van den Bulcke, J., and Thybring, E. E. (2022). "Moisture dynamics of wood-based panels and wood fibre insulation materials," *Front. Plant Sci.* 13. DOI: 10.3389/fpls.2022.951175

Donato, I. D., and Lazzara, G. (2012). "Porosity determination with helium pycnometry as a method to characterize waterlogged woods and the efficacy of the conservation treatments," *Archaeometry* 54(5), 906-915. DOI: 10.1111/j.1475-4754.2011.00657.x

Euring, M., Kirsch, A. A., and Kharazipour, A. (2015). "Hot-air/hot-steam process for the production of laccase-mediator-system bound wood fiber insulation boards," *BioResources* 10(2), 3541-3552. DOI: 10.15376/biores.10.2.3541-3552

Faghri, A., and Zhang, Y. (2006). *Transport Phenomena in Multiphase Systems with Phase Change*, Academic Press, Cambridge, MA, USA. Hameury, S. (2005). "Moisture buffering capacity of heavy timber structures directly exposed to an indoor climate: A numerical study," *Build. Envir.* 40(10), 1400-1412. DOI: 10.1016/j.buildenv.2004.10.017

Karagiozis, A., Künzel, H., Holm., A., and WUFI. (2001). *WUFI-ORNL/IBP Hygrothermal Model. Buildings VIII/Moisture Model Inputs—Principles.*

Kermani, A. (2006). Performance of structural insulated panels. *Proceedings of the Institution of Civil Engineers - Structures and Buildings*, 159(1), 13–19. https://doi.org/10.1680/stbu.2006.159.1.13

Kirsch, A., Ostendorf, K., and Euring, M. (2018). "Improvements in the production of wood fiber insulation boards using hot-air/hot-steam process," *European Journal of Wood and Wood Products* 76(4), 1233-1240. DOI: 10.1007/s00107-018-1306-z

Koizumi, Y., Shoji, M., Monde, M., Takata, Y., and Nagai, N. (2017). *Boiling*, Elsevier, Amsterdam.

Kunič, R. (2017). "Carbon footprint of thermal insulation materials in building envelopes," *Energy Efficiency* 10(6), 1511-1528. DOI: 10.1007/s12053-017-9536-1

Lawrence, M., Shea, A., Walker, P., and De Wilde, P. (2013). "Hygrothermal performance of bio-based insulation materials," *Proceedings of the Institution of Civil Engineers - Construction Materials* 166(4), 257-263. DOI: 10.1680/coma.12.00031

Meissner, J. W., Mendes, N., Mendonça, K. C., and Moura, L. M. (2010). "A full-scale experimental set-up for evaluating the moisture buffer effects of porous material," *Int. Commun. Heat Mass.*, 37(9), 1197-1202. DOI: 10.1016/j.icheatmasstransfer.2010.07.022

Muthuraj, R., Lacoste, C., Lacroix, P., and Bergeret, A. (2019). "Sustainable thermal insulation biocomposites from rice husk, wheat husk, wood fibers and textile waste fibers: Elaboration and performances evaluation," *Industrial Crops and Products* 135, 238-245. DOI: 10.1016/j.indcrop.2019.04.053

O'Dwyer, J., Walshe, D., and Byrne, K. A. (2018). "Wood waste decomposition in landfills: An assessment of current knowledge and implications for emissions reporting," *Waste Manag.* 73, 181-188. DOI: 10.1016/j.wasman.2017.12.002

Osanyintola, O. F., and Simonson, C. J. (2006). "Moisture buffering capacity of hygroscopic building materials: Experimental facilities and energy impact," *Energ. Build.*, 38(10), 1270-1282. DOI: 10.1016/j.enbuild.2006.03.026

Pacheco-Torgal, F., Jalali, S., and Fucic, A. (2012). *Toxicity of Building Materials*, Woodhead Publishing.

Palumbo, M., Lacasta, A. M., Holcroft, N., Shea, A., and Walker, P. (2016). "Determination of hygrothermal parameters of experimental and commercial bio-based insulation materials," *Constr. Build. Mater.* 124, 269-275. DOI: 10.1016/j.conbuildmat.2016.07.106

Rose, W. B. (1992). "Measured values of temperature and sheathing moisture content in residential attic assemblies," in: *Proceedings of the ASHRAE/DOE/BTECC Conference*, Clearwater Beach, FL, USA.

Salonvaara, M. (2004). "Moisture buffering effects on indoor air quality-experimental and simulation results," in: *Proceedings (CD) of the Performance of Exterior Envelopes of Whole Buildings IX International Conference*, Clearwater Beach, FL, USA.

Schiavoni, S., D′Alessandro, F., Bianchi, F., and Asdrubali, F. (2016). "Insulation materials for the building sector: A review and comparative analysis," *Renewable Sustainable Energy Rev.*, 62(62), 988-1011. DOI: 10.1016/j.rser.2016.05.045

Simonson, C. J., Salonvaara, M., and Ojanen, T. (2004a). "Heat and mass transfer between indoor air and a permeable and hygroscopic building envelope: Part I – Field measurements," *J. Therm. Envelope Build. Sci.* 28(1), 63-101. DOI: 10.1177/1097196304044395

Simonson, C. J., Salonvaara, M., and Ojanen, T. (2004b). "Moderating indoor conditions with hygroscopic building materials and outdoor ventilation," *ASHRAE Transactions* 110(2), 804-819.

Stec, A. A., and Hull, T. R. (2011). "Assessment of the fire toxicity of building insulation materials," *Energ. Buildings* 43(2-3), 498-506. DOI: 10.1016/j.enbuild.2010.10.015

TimberHP, & Go Lab Inc. 2024. (n.d.). "Assorted cuts of TimberBoard [Online Image]," Retrieved June 29, 2024, from https://www.timberhp.com/products/timberboard

Veitmans, K., and Grinfelds, U. (2016). "Wood fiber insulation material," *Research for Rural Development*, Vol. 2(ISSN 2255-923X), 91-98.

Vololonirina, O., Coutand, M., and Perrin, B. (2014). "Characterization of hygrothermal properties of wood-based products – Impact of moisture content and temperature," *Constr. Build. Mater.* 63, 223-233. DOI: 10.1016/j.conbuildmat.2014.04.014

Winandy, J. E., and Hatfield, C. A. (2007). "Analysis of three-year Wisconsin temperature histories for roof systems using wood, wood-thermoplastic composite, and fiberglass shingles," *For. Prod. J.* 57(9), 87-96.